

# Internal friction characterization of graphite

J. N. Wei · T. C. Huang · L. Zhao · J. M. Yu · W. J. Xie · G. M. Li

Received: 11 January 2008 / Accepted: 19 June 2008 / Published online: 16 July 2008  
© Springer Science+Business Media, LLC 2008

**Abstract** The effects of temperature on the damping behavior of bulk graphite were investigated and some novel phenomena were observed. The internal friction (IF) background of the bulk graphite has small temperature dependent and the IF value is much smaller than that of reported data. Moreover, two IF peaks were found in the IF-temperature spectrums. The first is proved to originate from the sweeping motion of in-plane dislocations and is a relaxation-type IF peak. The average activation energy of the peak is around  $1.10 \pm 0.06$  eV and the pre-exponential factor  $\tau_0$  is  $10^{-14}$  s. The second is a transformation peak, resulting from the transformation of asphalt that was used as binder in preparation of bulk graphite.

## Introduction

High damping materials allow undesirable mechanical vibration and wave propagation to be passively suppressed. This proves valuable in the control of noise and the enhancement of vehicle and instrument stability. Accordingly, the scientific community is continually working toward the development of high damping metals and high damping metal matrix composites (MMCs). The MMCs are particularly attractive in weight-critical applications when the matrix and reinforcement phases are combined to

provide desirable property combinations, such as high damping and low density. This class of materials, which incorporates a nonmetallic reinforcing phase into the matrix alloy, may exhibit high damping through the addition of reinforcing phases that possess high intrinsic damping or that dramatically modify the matrix microstructure [1–4]. More recently, particulate reinforced MMCs have shown promising improvements in damping and other mechanical properties [1–7]. Among the materials that are available as particulate reinforcement, SiC, Al<sub>2</sub>O<sub>3</sub>, and graphite particulates are most frequently used in MMCs. Graphite particulates, unlike SiC and Al<sub>2</sub>O<sub>3</sub> particulates, are found to exhibit a relatively high damping capacity when measured in its bulk form [8]. The addition of graphite particulates of various sizes to aluminum alloys has been proved to produce a substantial increase in damping capacity [6, 9–13]. However, we have, as yet, little understanding of what damping behavior the bulk graphite has and how the testing conditions influence this behavior. Undoubtedly, this knowledge is extremely important for us to understand the operative damping mechanism in graphite particulate reinforced MMCs. The objective of the present work was therefore to apply internal friction (IF) to the study of damping behavior of graphite. Damping measurements are carried out over a wide range of temperatures, frequencies, and strain amplitudes on the bulk graphite.

J. N. Wei (✉) · T. C. Huang · L. Zhao · J. M. Yu · W. J. Xie  
Department of Science, Jiujiang University, Jiujiang,  
Jiangxi 332005, China  
e-mail: cl\_weijianning@jju.edu.cn

G. M. Li  
Department of Mechanical Engineering, Jiujiang University,  
Jiujiang, Jiangxi 332005, China

## Experimental

Bulk graphite specimens in the present study were cut by electric sparking machine from graphite electrode used in arc furnace. During the fabrication of the electrode, some asphalt used as binder was mixed with the graphite

particulates. The density of the bulk graphite specimen studied in this work is  $1.72 \text{ g/cm}^3$ . The theoretical density of graphite is  $2.265 \text{ g/cm}^3$  [8]. The chip-shaped specimens were used for damping measurements that have a dimension of  $2.1 \times 2.5 \times 65.0 \text{ mm}^3$ .

The multifunctional internal friction apparatus (MFIFA) was used to measure the damping capacity and relative dynamic modulus of the bulk graphite through forced vibration [3]. This apparatus consists, basically, of an inverted torsion pendulum, a temperature programmer, and a photoelectron transformer. An IBM PC486 computer and an 8087 processor control the whole measurement, and the data can be processed in real time. The calculations of the inverse quality factor  $Q^{-1}$  and the relative dynamic modulus by the MFIFA is based on the following forced vibration equation:

$$m \frac{d^2x}{dt^2} + k^*x = F \tag{1}$$

$$k^* = k_1 + ik_2 = k_1(1 + i \tan \phi), \tag{2}$$

where  $m$  denotes the vibrating system mass,  $x$  the displacement,  $t$  the time,  $k^*$  the elastic constant,  $F$  the external sinusoidal time-varying force,  $k_1$  and  $k_2$  the real and imaginary parts of the complex modulus of the specimen, respectively, and  $\tan \phi$  the loss tangent. From the values of  $k_1$  and  $k_2$ , the damping capacity  $Q^{-1}$  is calculated by:

$$Q^{-1} = \tan \phi = \frac{k_2}{k_1} \tag{3}$$

We define the complex shear modulus  $G^*(\omega)$  by

$$G^*(\omega) = \tau/\gamma = |G|(\omega)e^{i\phi(\omega)} \tag{4}$$

$$G^*(\omega) = G_1(\omega) + iG_2(\omega) \tag{5}$$

$$|G| = \sqrt{G_1^2 + G_2^2}. \tag{6}$$

where  $\omega$  is the circular frequency of vibration,  $\tau$  the relative shear stress,  $\gamma$  the relative shear strain,  $\phi$  the angle by which the relative shear strain lags behind the relative shear stress,  $G_1(\omega)$  and  $G_2(\omega)$  are, respectively, the real and imaginary parts of  $G^*(\omega)$ , and  $|G|$  the relative dynamic modulus. During the temperature cycle, the specimen was oscillated at five discrete frequencies of 0.5, 1.0, 2.0, 3.0, and 4.0 Hz in sequence. The range of the maximum excitation torsional strain amplitude is  $10 \times 10^{-6}$  to  $40 \times 10^{-6}$ . The resolution of the IF measurement is  $10^{-4}$ .

**Results and discussion**

Figure 1 shows the changes of internal friction and relative dynamic modulus for bulk graphite specimen over the

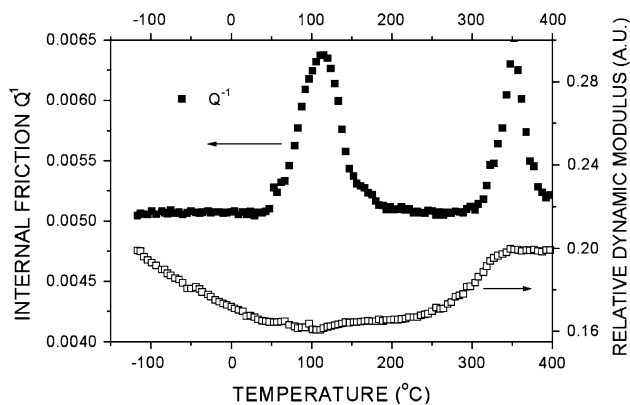


**Fig. 1** Dependence of IF and relative dynamic modulus of bulk graphite on temperatures (measuring frequency: 1.0 Hz)

temperature range of  $-120-400 \text{ }^\circ\text{C}$ . Several interesting trends may be noted in the figure. The most significant feature is that two IF peaks can be clearly seen in the IF curve. Excepting the peaks, the IF background has small temperature dependent. Corresponding to the position of the low-temperature IF peak, the modulus decreases to a minimum value, which is close to the abnormal modulus effect [3, 5, 8], but no modulus change can be found at the position of the high-temperature IF peak. These results, particularly IF peaks, are quite different from those reported by other investigators [8]. There is no peak reported in their work. We will discuss the mechanisms of the IF peaks in the following sections.

To clarify the mechanisms of the two IF peaks, we carried out further investigations. As shown in Fig. 2, the low-temperature IF peak is frequency dependent, i.e., the peak position shifts toward higher temperature with increasing measuring frequency. It is clear that the peak is relaxational type, and can be proved in following sections to relate to the intrinsic damping characterization of graphite. According to the fitted results to the theory of

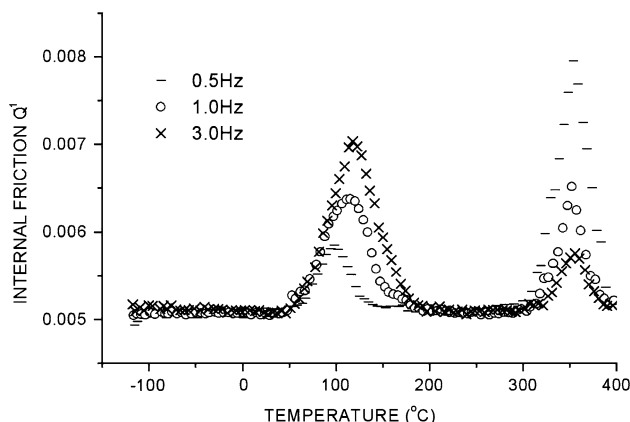


**Fig. 2** Influence of frequency on the position of low-temperature IF peak

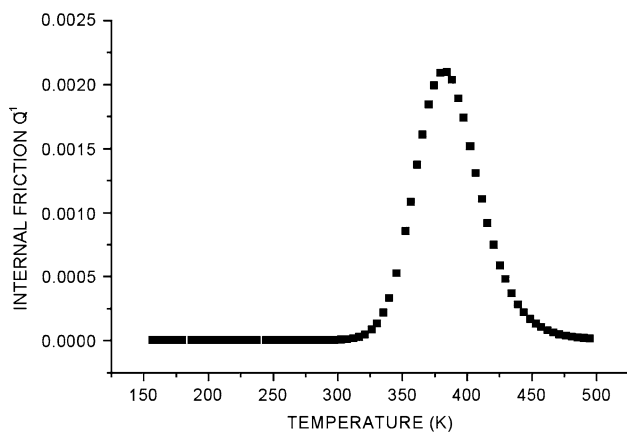


**Fig. 3** Low-temperature IF peak after deducting the IF background (measuring frequency: 1.0 Hz)

Arrhenius (using the frequency and the peak temperature) [14], the activation energy associated with this relaxation process is  $1.10 \pm 0.06$  eV and the pre-exponential factor  $\tau_0$  is  $10^{-14}$  s. Figure 3 shows that the low-temperature IF peak with subtracting IF background [14]. From Fig. 3, we can calculate that the low-temperature IF peak has a peak half width about  $2.08 \times 10^{-4}$ , which is very close to the theoretical value  $2.04 \times 10^{-4}$  [14]. Further experiments showed that the low-temperature IF peak is strain independent within the low-strain amplitudes ranging from  $10 \times 10^{-6}$  to  $40 \times 10^{-6}$ . The mechanism of this peak can be understood from the structure of graphite. The hexagonal lattice structure of ideal single crystal graphite consists of parallel hexagonal net planes in an ABABA stacking sequence. The strong in-plane covalent bonding and weak van der Waals through-plane forces lead to a large degree of anisotropy. This anisotropy can facilitate sliding between graphite basal planes [15]. Under cyclic loading, this sliding induces friction losses attributed largely to the dislocation mechanism proposed by Granato and Lücke [16]. This mechanism, based on the sweeping motion of dislocations from pinning points, is believed to occur in the high concentration of glissile basal plane dislocations found in graphite [8]. As we know, during the specimen fabrication process, some amorphous (glass) carbon formed and precipitated, acting as pinning points for the dislocations. Equation 7 can be used to describe the dislocation vibrating-string mechanism [17].

$$\tan \phi \approx \frac{\Lambda^2 b^2}{12\gamma J_U} \frac{\omega\tau}{[1 - (\omega^2/\omega_0^2)]^2 + \omega^2\tau^2} \quad (7)$$

where  $\tan \phi$  represents IF,  $\Lambda$  the dislocation density,  $l$  a dislocation loop of length pinned firmly at its ends,  $b$  the magnitude of the Burgers vector,  $\omega$  the angular frequency of stress variation,  $\tau$  the relaxation time,  $\gamma$  the effective line tension of the dislocation,  $J_U$  the compliance of the perfect

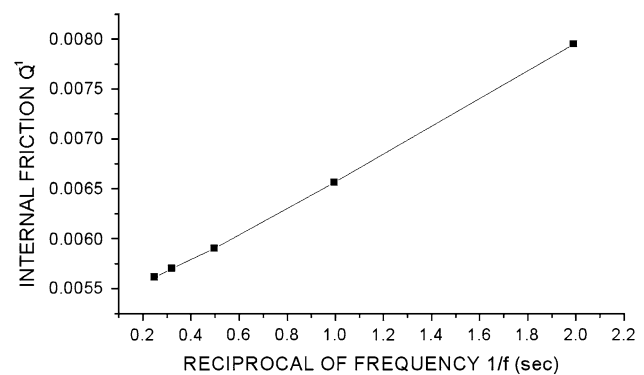


**Fig. 4** The relationship of the height of high-temperature IF peak with reciprocal of frequency

crystal, and  $\omega_0$  the resonant frequency. In generally,  $\omega_0/2\pi$  is on the order of  $10^9$  Hz for reasonable numbers for physical constants [17]. This is higher than the frequencies employed experimentally in the present work. While  $\omega \ll \omega_0$ , i.e.,  $\tau \gg 1/\omega_0$ ,  $\tan \phi$  takes on the form of a Debye peak with maximum at  $\omega\tau = 1$ .

According to the phase diagram [8], asphalt is a complex composite, which consists of various aromatic compounds. A chemical condensation reaction will take place at about 350 °C and a stable intermediate or liquid crystal will form [15]. Figure 1 shows that the high-temperature IF peak appears at around 350 °C, which is consistent with the transformation temperature. In order to determine the origin of the peak, further experiments were carried out. From Fig. 2, it is shown that the height of the high-temperature IF peak is roughly inversely proportional to vibration frequency. In fact, the height of the peak is linear with vibration reciprocal of frequency, as shown in Fig. 4. As is known, any transformation is more or less influenced by the velocity of temperature change. From Fig. 5, it is quite clear that the height of the high-temperature IF peak increases with increasing heating velocity which is consistent with Delorme Model [18]:

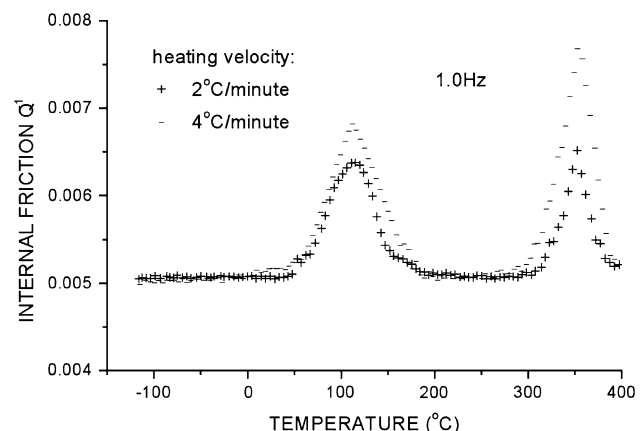


**Fig. 5** The effects of heating velocity on the high-temperature IF peak

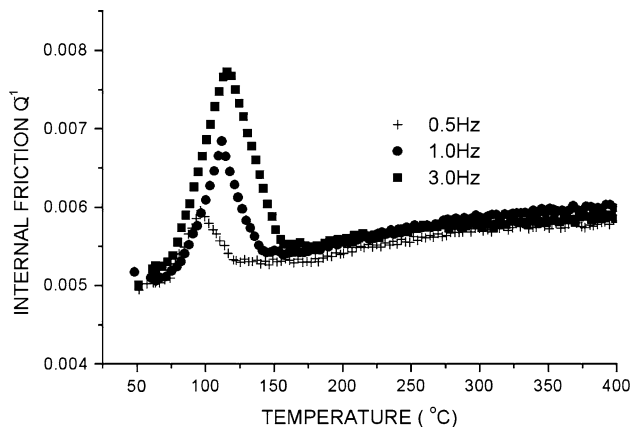


**Fig. 6** Dependence of IF of bulk graphite on temperatures, annealed at 1,200 °C for 2 h

$$\delta = \frac{A}{2} \left( \frac{dM}{dT} \cdot \frac{\dot{T}}{f} \right) \quad (8)$$

where  $\delta$  is IF ( $\delta = \pi Q^{-1}$ ),  $A$  the material constant,  $dM$  the increment of martensite with temperature change  $dT$ ,  $\dot{T}$  the heating velocity, and  $f$  the vibration frequency. All the results mentioned above prove that the high-temperature IF peak is a phase transformation peak.

The other strong evidence for the mechanisms of the peak is shown in Fig. 6. Before measured, the chip-shaped specimen is annealed for 2 h at 1,200 °C in order to eliminate asphalt. In Fig. 6, the high-temperature IF peak disappears from IF curve, while the low-temperature IF peak still appears, which makes clear that the high-temperature IF peak is an asphalt transformation peak and the low-temperature IF peak is a dislocation peak.

The low-temperature IF peak of graphite makes the damping capacity of MMCs rapidly increase with increasing temperature within the low temperatures, as was observed in our studying work [19, 20]. The difference between the coefficient of thermal expansion (CTE) between the matrix and the reinforcement results in dislocations generated at the interfaces during cooling and solidification of MMCs. Consequently, this becomes a possible source of high internal friction because of the motion of the dislocations under cyclic loading. In all, the results obtained in the present work will improve our understanding of the damping behavior and operative mechanisms of MMCs, and will give some useful information on their applications.

## Conclusions

In summary, the damping behavior of bulk graphite has been characterized by internal friction-temperature spectrum. Some interesting results were obtained. At low temperatures (below 100 °C), the dynamic modulus decreases with

increasing temperature, while at high temperatures, dynamic modulus exhibits an abnormal behavior. The internal friction measurements ( $Q^{-1}$ ) are 0.005 to 0.008 over temperature ranging  $-120$ – $400$  °C at 3.0 Hz. The IF value is much smaller than those reported by other researchers [8]. In particular, two IF peaks were detected in the IF-temperature curves. Experimental results showed that the IF background of bulk graphite has small temperature dependent. The low-temperature IF peak is attributed to the motion of dislocations. Its activation energy is  $1.10 \pm 0.06$  eV and pre-exponential factor  $\tau_0$  is  $10^{-14}$  s. The high-temperature IF peak originates from phase transformation of asphalt.

**Acknowledgements** The authors are grateful to the Jiangxi Province Natural Science Foundation of China (ratification No: 0550050) and the Jiangxi Provincial Department of Education Foundation of China (ratification No: 13-3-B-04) for the financial support.

## References

- Everett RK, Arsenault RJ (1991) Metal matrix composites processing and interfaces. Academic Press, Boston, MA, p 3
- Taya M, Arsenault RJ (1989) Metal matrix composites thermo-mechanical behavior. Pergamon Press, Oxford, p 126
- Wei JN, Cheng HF, Gong CL, Han FS, Shui JP (2002) *Metab Mater Trans A* 33:3565. doi:10.1007/s11661-002-0344-6
- Rawal SP, Misra MS (1986) In: Rath BB, Misra MS (eds) Role of interfaces on material damping. ASM, Materials Park, Ohio, p 18
- Updike CA, Bhagat RB, Pechersky MJ, Amateau MF (1990) *J Met* 42:42
- Rohatgi PK, Asthan R, Kumar A, Nath D, Shroeff S (1988) In: Fishman SG, Dhingra AK (eds) Cast reinforced metal composite. ASM, Materials Park, Ohio, p 264
- Taya M (1991) *Mater Trans JIM* 32:1
- Kelly BT (1981) *Physics of graphite*. Appl Sci Publ, London, p 8
- Rohatgi PK, Murali N, Shetty HR, Chandrashekar R (1976) *Mater Sci Eng* 26:115. doi:10.1016/0025-5416(76)90233-0
- Zhang J, Perez RJ, Gungor MN, Lavernia EJ (1992) In: Upadhya K (ed) Developments in ceramic and metal-matrix composites. TMS, Warrendale, PA, p 107
- Zhang J, Perez RJ, Gungor MN, Lavernia EJ (1993) In: Bhagat RB (ed) Damping of multiphase inorganic materials. AMS International, Materials Park OH, p 127
- Zhang J, Perez RJ, Gungor MN, Lavernia EJ (1993) *Scr Metall Mater* 28:91. doi:10.1016/0956-716X(93)90543-2
- Perez RJ, Zhang J, Lavernia EJ (1991) Proceedings of 17th Int. Symp For Testing and Failure Analysis, ISTFA/91. ASM International, Materials Park, OH, p 445
- Bevington PR (1969) *Data reduction and error analysis for the physical science*. McGraw-Hill, New York, p 26
- Delmonte J (1981) Technology of carbon and graphite fiber composites. Van Nostrand Reinhold Company, p 6
- Granato A, Lücke K (1981) *J Appl Phys* 52:7136. doi:10.1063/1.328687
- Nowick AS, Berry BS (1972) *Anelastic relaxation in crystalline solids*. Academic Press, New York, p 28
- Delorme JE, Gobin PF (1973) *Metaux corrosion-industrie* 573:185
- Wei JN, Wang DY, Xie WJ, Luo JL, Han FS (2007) *Phys Lett A* 366:134. doi:10.1016/j.physleta.2007.01.061
- Wei JN, Li YL, Song SH, Ji GC, Ma ML, Zhang DQ (2004) *Phys Status Solid* 201:923. doi:10.1002/pssa.200306778